

Synthesis of Arrayed, TiO₂ Needlelike Nanostructures via a Polystyrene-*block*-poly(4-vinylpyridine) Diblock Copolymer Template

Chin-Cheng Weng, Kuo-Feng Hsu, and Kung-Hwa Wei*

Department of Materials Science and Engineering, National Chiao Tung University,
Hsinchu, Taiwan 30049, Republic of China

Received April 19, 2004. Revised Manuscript Received August 10, 2004

Arrayed, needlelike nanostructures of rutile phase crystal TiO₂ were grown on a Si substrate containing TiO₂ seeds prepared through a thin polystyrene-*b*-poly(4-vinylpyridine) (PS-*b*-P4VP) diblock copolymer template. The morphology of the deposited TiO₂ nanostructures was characterized by field-emission scanning electron microscopy, X-ray diffraction, and transmission electron microscopy (TEM). By using TiO₂ seeds prepared from their diblock copolymer PS-*b*-P4VP template, we fabricated arrayed, needlelike rutile TiO₂ nanostructures with variable spatial positions and densities. The distance between two TiO₂ needle bunches (120 and 160 nm) could be controlled using block copolymer templates with different molecular weights.

Introduction

Titanium dioxide (TiO₂) is a highly versatile material, because of the optical and catalytic properties exhibited by its two common crystal forms: rutile and anatase. The rutile phase of TiO₂ has a high refractive index and is useful for optical devices, such as waveguides.¹ The photocatalytic activity of the anatase phase of TiO₂ is widely applied in many fields, such as microorganism photolysis,² medical treatment,³ environmental purification,⁴ and photovoltaic cells.^{5,6} More recently, ordered nanostructures have been prepared using templating techniques. For example, ordered TiO₂ nanotubes were synthesized using porous anodic alumina as templates via a sol–gel process.^{7–12} TiO₂ nanowire arrays have also been synthesized using an electrochemical method.¹³

On the other hand, the fabrication of periodically ordered two-dimensional nanostructures on the scale of tens to hundreds of nanometers is critically important as electronic, optical, and magnetic devices are continually miniaturized. Attempts have been taken to arrange nanomaterials, such as semiconductor nanocrystals, as well as metal and metal oxide nanoparticles, into ordered structures for device applications.^{14–17} A diblock copolymer chain consists of two chemically dissimilar

blocks attached through a covalent bond. These diblock copolymers can microphase separate into various ordered nanostructures with periodic thicknesses between 10 and 100 nm.¹⁸ Thin films of diblock copolymers can therefore be used as lithographic templates to produce highly dense nanostructures^{19–22} or as nanoreactors for the synthesis of nanocrystal clusters with spatial control.^{23–27} Quasi-regular arrays of Au clusters,^{23,24} Co and Fe arrays,²⁵ and self-assembly of both Au and Fe₂O₃

(7) Hoyer, P. *Langmuir* **1996**, *12*, 1411.

(8) Lakshmi, B. B.; Dorhout, P. K.; Martin, C. R. *Chem. Mater.* **1997**, *9*, 857.

(9) Lakshmi, B. B.; Patrissi, C. J.; Martin, C. R. *Chem. Mater.* **1997**, *9*, 2544.

(10) Zhang, X. Y.; Zhang, L. D.; Chen, W.; Meng, G. W.; Zheng, M. J.; Zhao, L. X. *Chem. Mater.* **2001**, *13*, 2511.

(11) Liu, S. M.; Gan, L. M.; Liu, L. H.; Zhang, W. D.; Zeng, H. C. *Chem. Mater.* **2002**, *14*, 1391.

(12) Lei, Y.; Zhang, L. D.; Meng, G. W.; Li, G. H.; Zhang, X. Y.; Liang, C. H.; Cheng, W.; Wang, S. X. *Appl. Phys. Lett.* **2001**, *78*, 1125.

(13) Miao, Z.; Xu, D.; Ouyang, J.; Guo, G.; Zhao, X.; Tang, Y. *Nano Lett.* **2002**, *2*, 717.

(14) Forster, S.; Antonietti, M. *Adv. Mater.* **1998**, *10*, 195.

(15) Lazzari, M.; Lopez-Quintela, M. A. *Adv. Mater.* **2003**, *19*, 1583.

(16) Park, C.; Yoon, J.; Thomas, E. L. *Polymer* **2003**, *44*, 6725.

(17) Tokuhisa, H.; Hammond, P. T. *Langmuir* **2004**, *20*, 1436.

(18) Reiter, G.; Castelein, G.; Sommer, J.-U.; Rolfele, A.; Thurn-Albrecht, T. *Phys. Rev. Lett.* **2001**, *87*, 226101.

(19) Park, M.; Harrison, C.; Chaikin, P. M.; Register, R. A.; Adamson, D. H. *Science* **1997**, *276*, 1401.

(20) Shin, K.; Leach, K. A.; Goldbach, J. T.; Kim, D. H.; Jho, J. Y.; Tuominen, M.; Hawker, C. J.; Russell, T. P. *Nano Lett.* **2002**, *2*, 933.

(21) Cheng, J. Y.; Ross, C. A.; Chan, V. Z.-H.; Thomas, E. L.; Lammertink, R. G. H.; Vancso, G. J. *Adv. Mater.* **2001**, *13*, 1174.

(22) Lopes, W. A.; Jaeger, H. M. *Nature* **2001**, *414*, 735.

(23) Haupt, M.; Miller, S.; Glass, R.; Arnold, M.; Sauer, R.; Thonke, K.; Moller, M.; Spatz, J. P. *Adv. Mater.* **2003**, *15*, 829.

(24) Spatz, J. P.; Mosser, S.; Hartmann, C.; Moller, M.; Herzog, T.; Krieger, M.; Boyen, H. G.; Ziemann, P.; Kabius, B. *Langmuir* **2000**, *16*, 407.

(25) Abes, J. I.; Cohen, R. E.; Ross, C. A. *Chem. Mater.* **2003**, *12*, 1125.

* To whom correspondence should be addressed. Telephone: 886-35-731871. Fax: 886-35-724727. E-mail: khwei@cc.nctu.edu.tw.

(1) Joannopoulos, J. D.; Villeneuve, P. R.; Fan, S. *Nature* **1997**, *386*, 143.

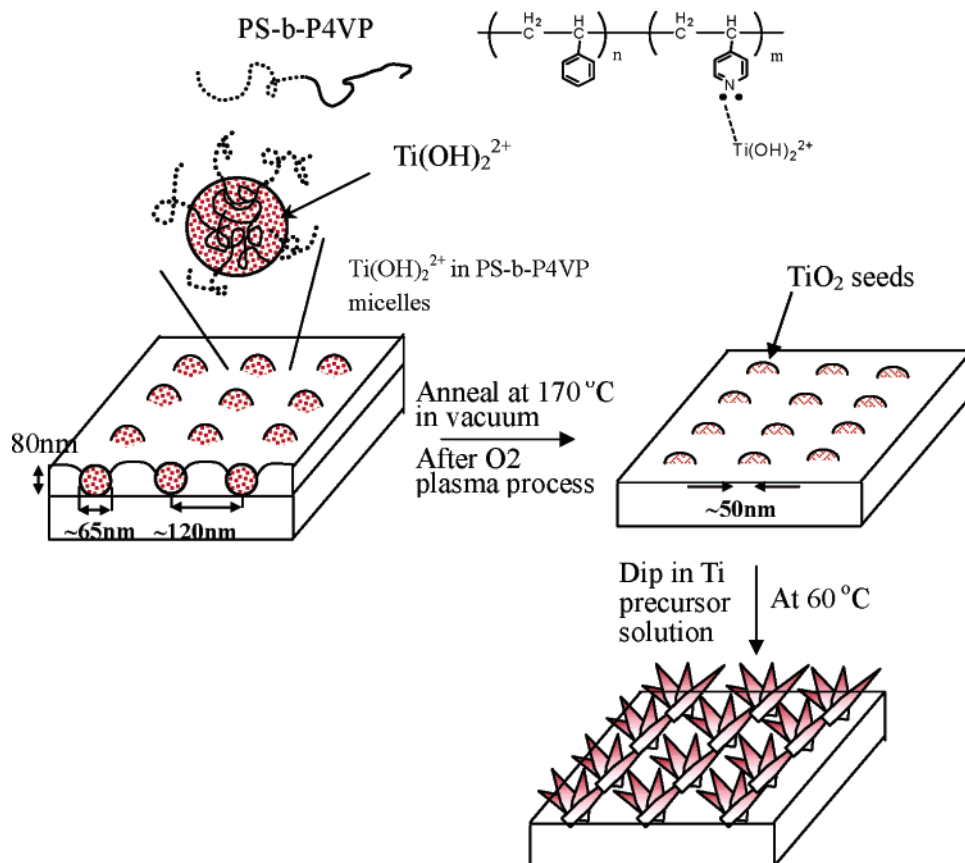
(2) Sunada, K.; Kikuchi, Y.; Hashimoto, K.; Fujishima, A. *Environ. Sci. Technol.* **1998**, *32*, 726.

(3) Cai, R.; Kubota, Y.; Shuin, T.; Hashimoto, K.; Fujishima, A. *Cancer Res.* **1992**, *52*, 2346.

(4) Hoffmann, M. R.; Martin, S. T.; Choi, W.; Bahnemann, D. W. *Chem. Res.* **1995**, *95*, 69.

(5) O'Regan, B. C.; Lenzmann, F. *J. Phys. Chem. B* **2004**, *108*, 4342.

(6) Jeon, S.; Braun, P. V. *Chem. Mater.* **2003**, *15*, 1256.

Scheme 1. Synthesis of Needlelike TiO₂ Nanostructures with Ordered Patterns

nanoparticles²⁶ have been synthesized using micellar polystyrene-*b*-poly(4-vinylpyridine) (PS-*b*-P4VP). Alternatively, presynthesized nanoparticles can be selectively dispersed in one block of a diblock copolymer using specific interactions between their surface ligands and the block. For instance, presynthesized CdS nanoparticles have been selectively incorporated in the PEO phase of polystyrene-*b*-poly(ethylene oxide) (PS-*b*-PEO) via dipole–dipole interactions.²⁷ In another case, surface-modified TiO₂ has been dispersed selectively into the PS or PMMA domain of polystyrene-*b*-poly(methyl methacrylate) (PS-*b*-PMMA), depending on the hydrophobic or hydrophilic nature of the surfactant.²⁸

In the present study, we report the synthesis of an arrayed TiO₂ nanostructure using ordered TiO₂ seeds, which were synthesized and incorporated into one block of a thin PS-*b*-P4VP nanotemplate. To our knowledge, this is the first time TiO₂ nanostructures have been grown using TiO₂ seeds. Scheme 1 demonstrates how the nanostructure is produced. This approach is particularly useful for controlling the density and spatial location of the TiO₂ nanostructures. The approach begins by incorporating Ti(OH)₂²⁺ ions selectively into one block (P4VP) of the diblock copolymer (PS-*b*-P4VP)

through ionic–polar interactions. Next, Ti(OH)₂²⁺ ions in the P4VP block order into TiO₂ seeds after thermal annealing. O₂ plasma treatment of the TiO₂/PS-*b*-P4VP was used to remove the polymer template. The TiO₂ molecules then crystallize on the TiO₂ seeds to form a needlelike TiO₂ nanostructure immersed in Ti precursor solutions.^{29–32} The detailed growth mechanisms of TiO₂ in a Ti precursor solution have been reported by Yamabi et al.^{29,30} and Sathyamoorthy et al.³¹

Experimental Section

Material. Polystyrene-*block*-poly (4-vinylpyridine) (PS-*b*-P4VP) diblock copolymer was purchased from Polymer Source, Inc. Two kinds of PS-*b*-P4VP were used. The number-average molecular weights (M_n) of the PS and P4VP blocks for the first copolymer were 92 700 and 32 700 g/mol, respectively, with the ratio of the weight-average molecular weight (M_w) to M_n (polydispersity) equal to 1.13, as determined by size exclusion chromatography (SEC). This copolymer is referred to as SVP252 in the present study. M_n values for the PS and P4VP blocks in the second copolymer (termed SVP229) were 365 300 and 29 400 g/mol, respectively, with a M_w/M_n (polydispersity) ratio of 1.23. Titanium oxide sulfate hydrate (TiOSO₄·*x*H₂O, Riedel-de Haën), urea (98%, Showa), toluene (99% TEDIA), and HCl (36% Acros) were used in the study.

Synthesis of Ordered TiO₂ Seeds. Si wafers were cleaned ultrasonically with diluted nitric acid and ethanol for 1 h, respectively, and then were dried with nitrogen gas. Titanium

(26) Sohn, B. H.; Choi, J. M.; Yoo, S.; Yun, S. H.; Zin, W. C.; Jung, J. C.; Kanehara, M.; Hirata, T.; Teranishi, T. *J. Am. Chem. Soc.* **2003**, *125*, 6368.

(27) (a) Yeh, S. W.; Wei, K. H.; Sun, Y. S.; Jeng, U. S.; Liang, K. S. *Macromolecules* **2003**, *36*, 7903. (b) Jeng, U. S.; Sun, Y. S.; Lee, H. Y.; Hsu, C. H.; Liang, K. S.; Yeh, S. W.; Wei, K. H. *Macromolecules* **2004**, *37*, 4617.

(28) Weng, C. C.; Wei, K. H. *Chem. Mater.* **2003**, *15*, 2936.

(29) Yamabi, S.; Imai, H. *Chem. Mater.* **2002**, *14*, 609.

(30) Yamabi, S.; Imai, H. *Chem. Lett.* **2001**, 200.

(31) Sathyamoorthy, S.; Moggridge, G. D.; Hounslow, M. J. *Cryst. Growth Des.* **2001**, *1*, 123.

(32) Yang, H. G.; Zeng, H. C. *J. Phys. Chem. B* **2003**, *107*, 12244.

(33) Kandori, K.; Kon-no, K.; Kitahara, A. *J. Colloid Interface Sci.* **1988**, *122*, 78.

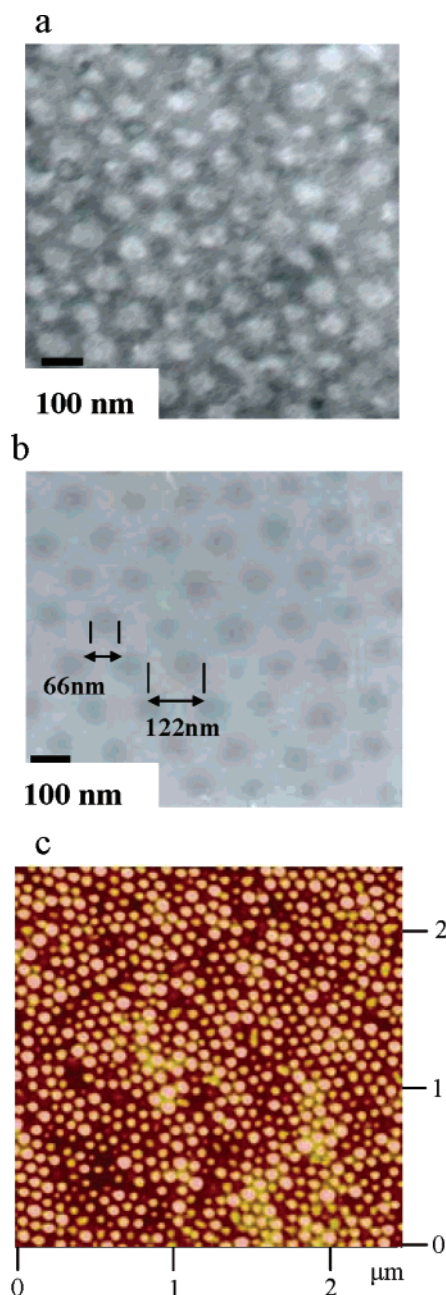


Figure 1. (a) Transmission electron microscopy image of SVP252 stained with RuO_4 , (b) transmission electron microscopy image, and (c) AFM topology in height images of a $\text{Ti}(\text{OH})_2^{2+}/\text{SVP252}$ ($P = 1$) thin film.

oxide sulfate hydrate was prehydrolyzed in deionized water to form $\text{Ti}(\text{OH})_2^{2+}$ in aqueous solution. SVP252 and SVP229 were dissolved in toluene at 70°C and cooled to room temperature to yield 0.5 and 0.2 wt % micellar solutions, respectively. By combining the $\text{Ti}(\text{OH})_2^{2+}$ aqueous solution with the PS-*b*-P4VP micelle solution, a $\text{Ti}(\text{OH})_2^{2+}/\text{PS-}b\text{-P4VP}$ solution was formed. The molar ratio of $\text{Ti}(\text{OH})_2^{2+}$ to P4VP was kept at 1 in this study. The weight ratio of the aqueous solution/toluene solution was held below 1.5×10^{-3} to keep the solution uniform. The resulting solution was subsequently stirred for 48 h, allowing the $\text{Ti}(\text{OH})_2^{2+}$ ions enough time to diffuse into the micelle cores and attach to the pyridine groups of P4VP through ionic–polar interactions. The micelle solutions remained transparent for 48 h. The maximum amount of $\text{Ti}(\text{OH})_2^{2+}$ allowed in the P4VP core was at $P = 2$ (P = molar ratio of $\text{Ti}(\text{OH})_2^{2+}$ to P4VP) to maintain solution uniformity. A monolayer film of PS-P4VP micelles with $\text{Ti}(\text{OH})_2^{2+}$ in P4VP was then fabricated by spin coating at 2500 rpm from the

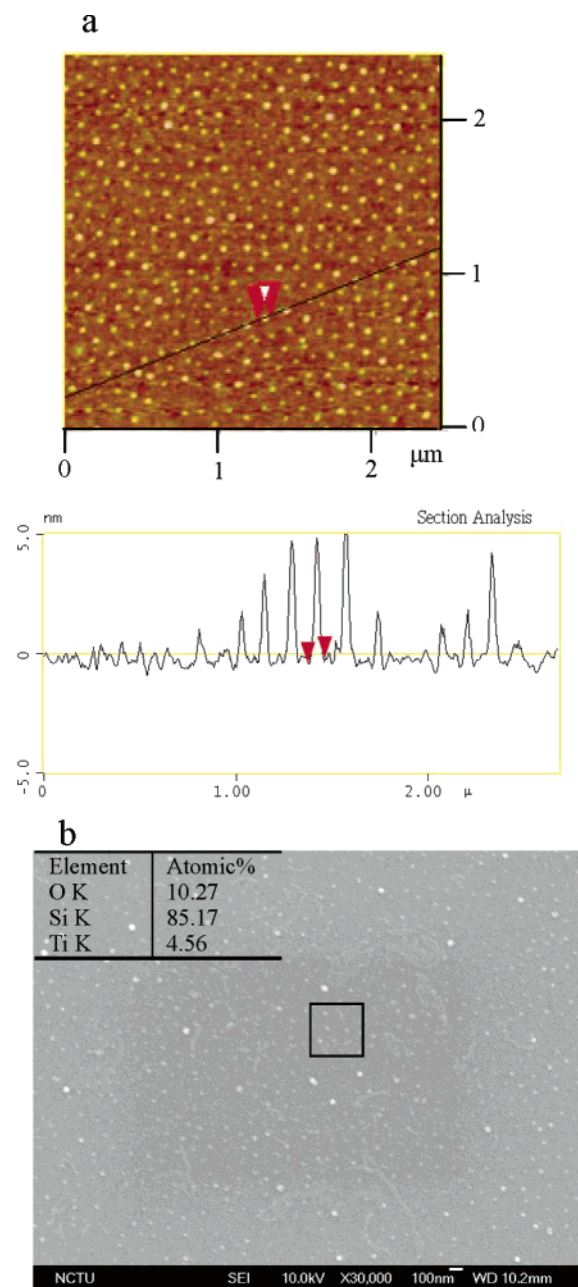
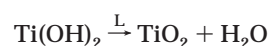
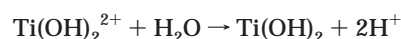


Figure 2. (a) AFM topology and line-section analysis of ordered TiO_2 seeds from a $\text{TiO}_2/\text{SVP252}$ ($P = 1$) thin film, and (b) SEM image of TiO_2 seeds from $\text{TiO}_2/\text{SVP252}$ (after O_2 plasma treating).

micellar solutions onto silicon wafers. The monolayer thin films were annealed at 170°C in a vacuum for 24 h. The $\text{Ti}(\text{OH})_2^{2+}$ ions condense into TiO_2 by the following reaction, as protons react with pyridine groups in PS-*b*-P4VP.



Subsequently, the polymer template was removed from the silicon wafer by plasma treating it at 110 W and 300 mTorr for 10 min. If more than 10 min are required for this step, TiO_2 seeds will be etched away. The TiO_2 that remains after plasma treatment is used to seed the growth of the TiO_2 nanostructures.

Synthesis of TiO_2 Needlelike Nanostructures. Precursor solutions with Ti concentrations of 0.0001–0.1 M were

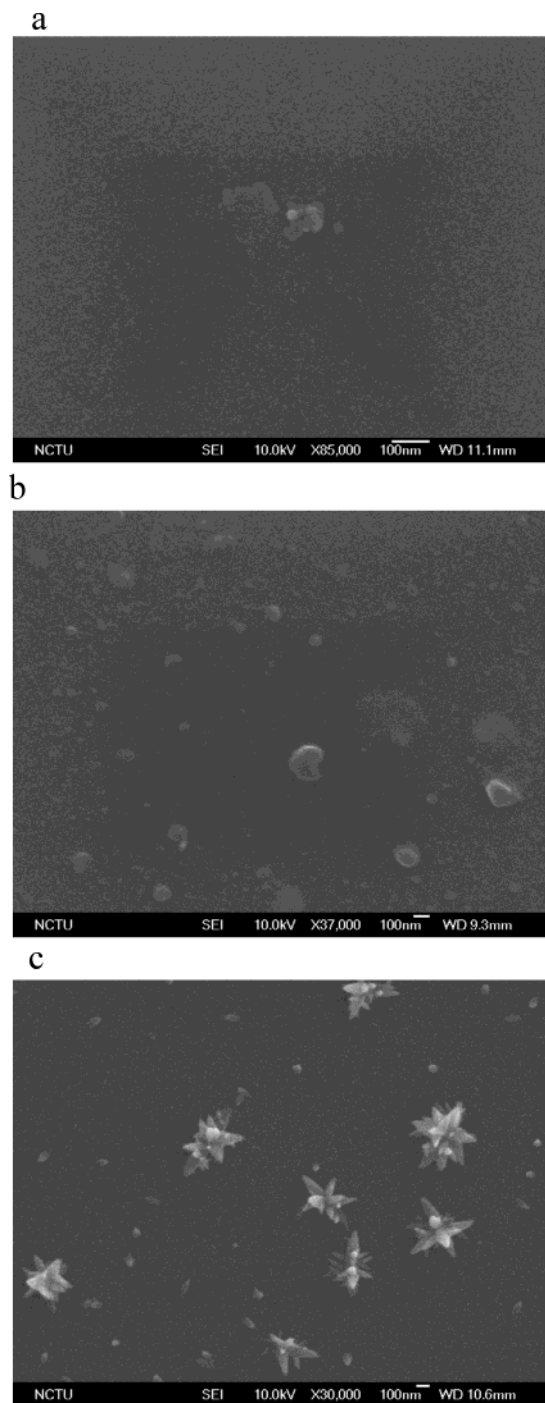


Figure 3. FE-SEM micrograph of TiO₂ deposited on a Si wafer without TiO₂ seeds in Ti precursor solution for (a) 1, (b) 6, and (c) 12 h.

prepared by adding TiOSO₄·xH₂O into aqueous solutions of hydrochloric acid (HCl) containing urea with an R molar ratio ($R = \text{urea}/\text{Ti}$) of 200 and were then stirred for approximately 1 h at room temperature. The initial pH value of the solutions was adjusted to 1 after 1 h of stirring. TiOSO₄ was chosen as a starting material because of its low cost, low reactivity with moisture, and lack of toxicity. Substrates were perpendicularly immersed into the precursor solutions and maintained at 60 °C. After an appropriate reaction time (30 min to 12 h), the substrates deposited with TiO₂ were rinsed with deionized water and dried at room temperature.

Characterization. Transmission electron microscopy (TEM) studies were carried out on a Hitachi H-600 electron microscope operating at 100 keV. The monolayer thin film was defined by the fact that the size of the P4VP core is close to

Table 1. Reaction Compositions of TiO₂ Nanostructures Deposited from Ti Precursor Solutions for 1 and 6 h with Ordered TiO₂ Seeds on the Si Substrate

sample name	PS- <i>b</i> -P4VP ^a	Ti concentration (M) (with urea $R^b = 200$)	reaction time (h)
252L1	SVP252	0.0001	1
252H1	SVP252	0.0005	1
229H1	SVP229	0.0005	1
252L6	SVP252	0.0001	6
252H6	SVP252	0.0005	6
229H6	SVP229	0.0005	6

^a Two kinds of block copolymers (SVP252 and SVP229) were used as templates in this study. ^b R is defined as the molar ratio of urea to Ti. The value is fixed at 200 in this study.

the thickness of the PS-*b*-P4VP thin film, which indicates that each thin PS-*b*-P4VP film only consists of one layer of P4VP cores. These films were removed from the Si wafer by etching the interface between the thin film and the Si-wafer with 1% HF solution. Subsequently, the self-standing films floating on water were deposited on a carbon-Cu grid for TEM studies. High-resolution transmission electron microscopy (HRTEM) studies were carried out on a JEOL 2010 electron microscope operating at 200 keV. An X-ray diffraction study was carried out with a MAC Science MXP 18 X-ray diffractometer (50 kV, 200 mA) with a copper target and Ni filter, at a scanning rate of 4 °C/min. Atomic force microscopy (AFM) measurements were performed in tapping-mode with a Digital Nanoscope IIIa under ambient conditions. Scanning electron micrography (SEM) and energy-dispersive X-ray scattering (EDX) data were obtained on a thermal field emission scanning electron microscope (JSM-6500F) with an accelerating voltage of 10 kV.

Results and Discussion

Figure 1a shows a TEM micrograph of a PS-*b*-P4VP/SVP252 thin film after staining with RuO₄. The micellar structure was constituted by the P4VP and PS blocks in the matrix, due to the selectivity of toluene solvent during the spin-coating process. The size of the P4VP sphere is about 65 nm, and the interdomain distance between P4VP spheres is about 125 nm. Figure 1b shows a transmission electron microscopy image of a Ti(OH)₂²⁺/SVP252 thin film at a molar ratio (P) of Ti to P4VP equal to 1. The dark region, which has high electron density, indicates that Ti(OH)₂²⁺ ions have been incorporated into the P4VP core of the micelles due to ionic–polar interactions. The distances between the nearest two cores (Ti(OH)₂²⁺/P4VP) and the cores sizes are similar for the different P ratios, implying that the concentration of Ti(OH)₂²⁺ does not affect the micelle size. Figure 1c shows the topology of a SVP252 monolayer thin film (the thickness of the thin film is only slightly larger than the size of the P4VP spheres (85 vs 65 nm)). The morphology of the Ti(OH)₂²⁺/SVP229 thin films is similar to that of Ti(OH)₂²⁺/SVP252, but with a difference; the distance between two micelles is 160 nm, and the film thickness is about 60 nm. Figure 2a shows the AFM topology in height images of TiO₂ seeds remaining on a silicon substrate after O₂ plasma treatment. In the image, the ordered TiO₂ seeds are 5 nm in height and 50 nm in width. For comparison, a monolayer thin film of SVP252 on a Si wafer was treated with O₂ plasma, and no remaining material could be detected. The average distance between two seeds is about 120 nm. Figure 2b displays an SEM image of a TiO₂/

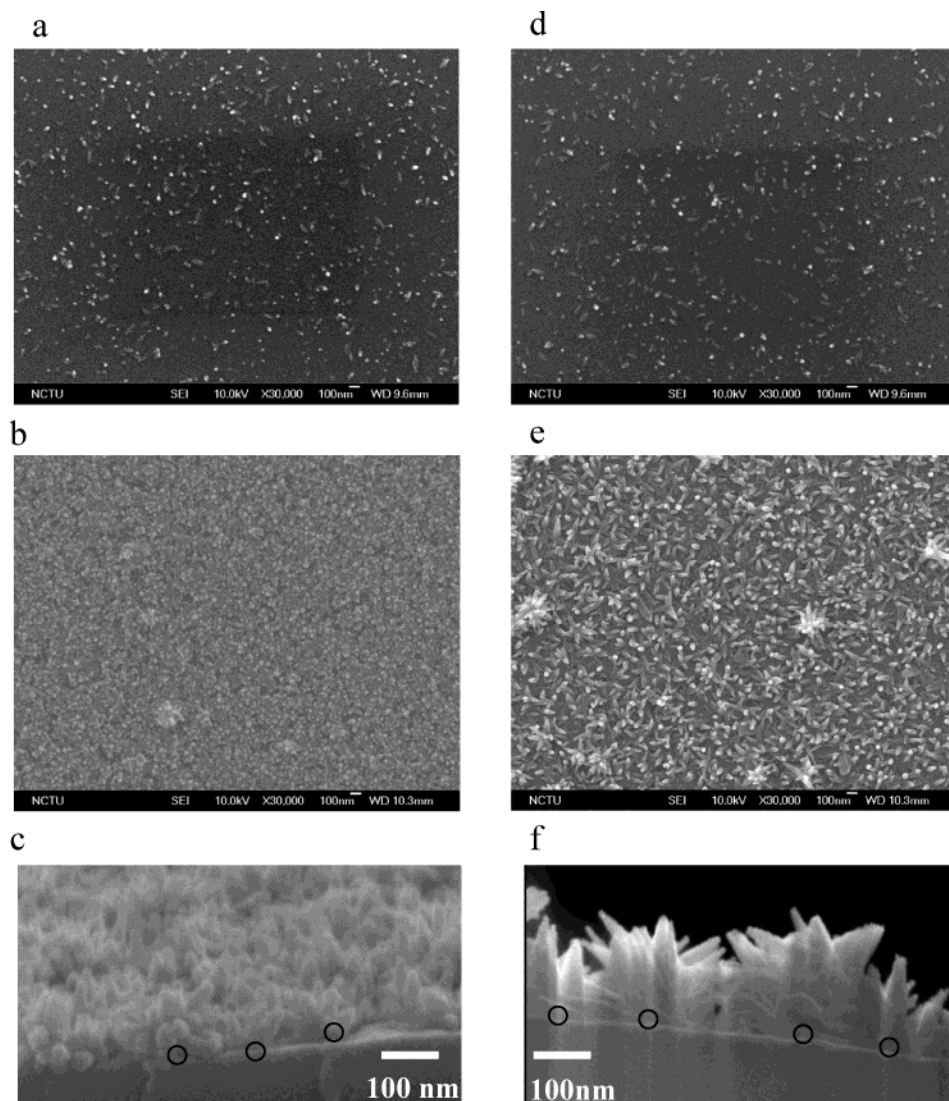


Figure 4. FE-SEM micrograph of TiO_2 seeds from $\text{TiO}_2/\text{SVP252}$ reacted in 0.0001 M Ti precursor solution for (a) 1 h (252L1) and (b) 6 h (252L6); (c) a cross-sectional profile of a 252L6 TiO_2 needle film; reacted in 0.0005 M Ti precursor solution for (d) 1 h (252H1) and (e) 6 h (252H6); and (f) a cross-sectional profile of a 252H6 TiO_2 needle film.

SVP252 thin film. The composition of the remaining TiO_2 seeds with short-range order was confirmed by EDS spectra. The ratio of the elemental percentage in the upper left-hand corner indicates that TiO_2 particles are present.

As a control experiment, Figure 3a–c shows SEM images of a pure Si wafer, without TiO_2 seeds, immersed in a 10^{-4} M Ti precursor solution for 1, 6, and 12 h, respectively. The images reveal that heterogeneous nucleation will occur on a blank Si wafer,³² but roughly 12 h is needed to form structured TiO_2 needles on Si substrates with Si–O–Ti bonds. The morphology of the TiO_2 films on Si substrates is similar to those observed by Yang et al.³² Table 1 provides the sample name and reaction conditions of films deposited from Ti precursor solutions onto various substrates for 1 and 6 h, respectively. Figure 4a shows an SEM image of a 10^{-4} M Ti precursor solution deposited with TiO_2 -seeded substrates for 1 h (252L1). Figure 4b displays an SEM image of TiO_2 short needles, 40–50 nm in length, after 6 h of growth (252L6). Figure 4c shows a cross-sectional profile of sample 252L6. The distance between the

nearest two bunches of needlelike TiO_2 is about 120 nm, similar to that for the TiO_2 seeds. When the precursor concentration is increased, the morphology becomes different. During the initial reaction stage, they are not easily distinguished. Figure 4d shows an SEM image of 252H1, which shows small islands of TiO_2 , similar to the case of 252L1. Figure 4e is an image revealing the long-needle structure. The length of the needles is about 130–150 nm. The tip of the needle for 252H6 is sharper than that for 252L6. From the cross-sectional profile image presented in Figure 4f, the tip size of the needle is about 3 nm. The needle length can be controlled by changing the growth parameters, such as reaction times or the reaction concentration. When the reaction time is fixed at short times such as in our cases, the growth of TiO_2 needles is controlled by the reaction kinetics, which affects the needles morphology. When using the PS-P4VP block copolymer templates at the same molecular weights, for example, in samples 252L6 and 252H6, the TiO_2 seeds density at per unit area are the same. Hence, as the concentration of Ti precursors increases, the reaction speed will increase accordingly,

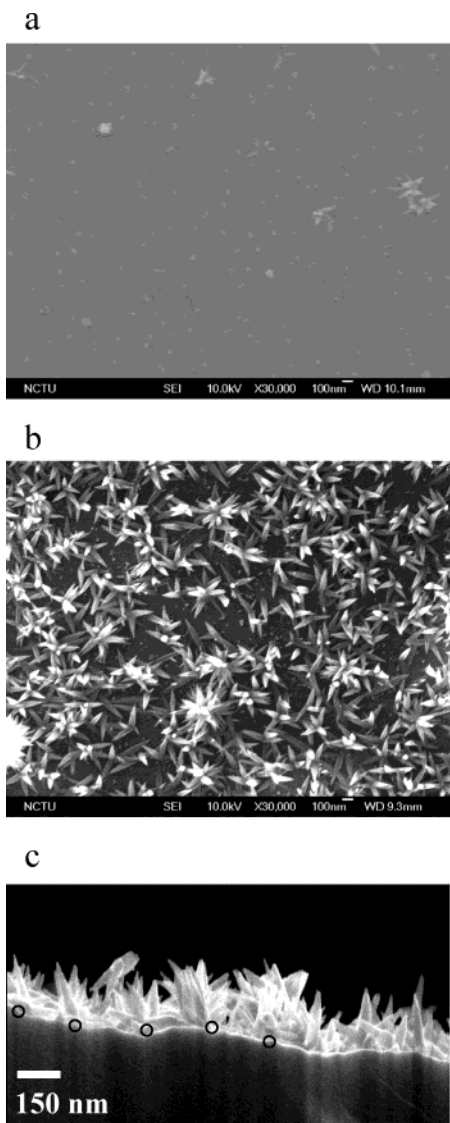


Figure 5. FE-SEM micrograph of TiO₂ seeds from TiO₂/SVP229 reacted in 0.0005 M Ti precursor solution for (a) 1 h (229H1) and (b) 6 h (229H6); and (c) a cross-sectional profile of a 229H6 TiO₂ needle film.

which in turn results in a larger size of TiO₂ needles. This is the reason the needle length and width of TiO₂ needles in the case of 252H6 are larger than those in the 252L6 case. Figure 5a and b shows an SEM image of TiO₂ seeds generated from a larger molecular weight PS-*b*-P4VP (SVP229) template; the seeds grow larger, and needle structures grow as the reaction time is increased to 6 h (229H6). Figure 5c shows a cross-sectional profile of sample 229H6. As compared to Figure 4f, the distance between the two needle bunches is larger (160 vs 120 nm). In the architecture of the PS-*b*-P4VP micelle, the P4VP blocks form the core while the PS blocks constitute the corona. When the molecular weight of the P4VP block differs only slightly in the diblock copolymers and the molecular weight of the PS block is much larger than that of P4VP block in the diblock copolymers, the distance between the P4VP cores is actually controlled by the size of or the molecular weight of the PS block. In the present study, the molecular weights of the P4VP blocks in SVP252 and SVP229 are 32 700 and 29 400 g/mol, respectively,

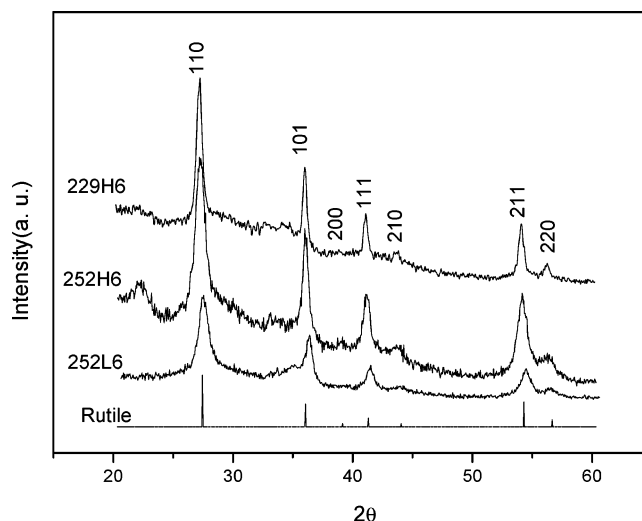


Figure 6. X-ray diffraction curves of 252L6, 252H6, and 229H6 TiO₂ needlelike nanostructures.

indicating that the domain size of the P4VP core in the thin films is roughly the same in two cases, whereas the molecular weights of the PS block in SVP252 and SVP229 are 92 700 and 365 300 g/mol, respectively. The distance between two P4VP cores in SVP229 is larger than that in SVP252. The structural variation in PS-*b*-P4VP is therefore used to vary the distance between the nucleation sites of TiO₂. This suggests that a variable density of TiO₂ nanostructures can be fabricated on a substrate using PS-*b*-P4VP block copolymer templates with different molecular weights.

Figure 6 shows diffraction peaks that can be indexed as the tetragonal rutile phase (JCPDS card File No. 75-1757). Figure 7a shows typical TEM images of the TiO₂ nanostructure, and Figure 7b shows a selective area electronic diffraction (SAED) pattern. Three typical diffraction spots are indexed as the 111, 110, and 220 planes by the ratio of $1/d_{hkl}$. From this TEM image, the needlelike TiO₂ nanostructure is observed to be more than 100 nm in length, terminating with a sharp pinnacle. An HRTEM image is shown in Figure 7c. It reveals that TiO₂ has a rutile crystal structure. The lattice spacing is about 3.2 Å between adjacent lattice planes of the TiO₂ needles, corresponding to the distance between (110) crystal planes of the rutile phase. The rutile and anatase crystals were formed at the condition near thermodynamic equilibrium of Ti(OH)₂²⁺/rutile and Ti(OH)₂²⁺/anatase, respectively.^{29,30} At low pH values or acidic conditions, the chemical potential of Ti(OH)₂²⁺ (μ_i) is slightly larger than that of the rutile phase (μ_r) and less than that of the anatase phase (μ_a). As a result, the rutile crystals are grown in the solution at pH values between 0.5 and 1.8. As the pH value increases, the anatase crystal will form in the solution instead by the fact that the μ_a value is slightly lower than μ_i ($\mu_r < \mu_i < \mu_a \rightarrow \mu_r < \mu_a < \mu_i$, as the pH value is increasing).

Conclusion

By using TiO₂ seeds prepared from a PS-*b*-P4VP diblock copolymer template, we have been able to

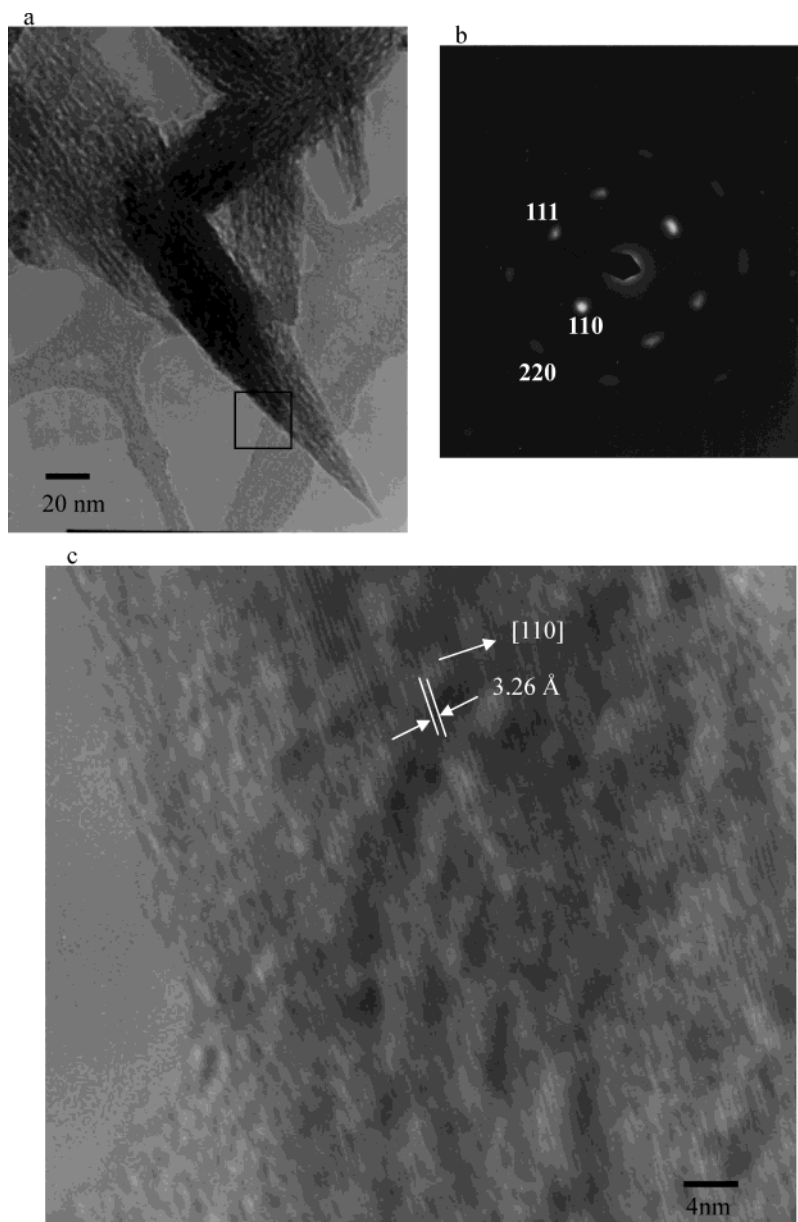


Figure 7. (a) TEM image, (b) electron diffraction pattern, and (c) HRTEM lattice image of the 252H6 TiO₂ needlelike nanostructure.

fabricate arrayed, needlelike rutile TiO₂ nanostructures with variable spatial positions and densities. The distance between two TiO₂ needle bunches (120 and 160 nm) can be controlled using block copolymer templates with different molecular weights.

Acknowledgment. We appreciate the financial support of the National Science Council, Taiwan, through project NSC 92-2120-M-009-009.

CM049367J